Inflow Seepage Influence on Pier Scour

STEVEN R. ABT, JERRY R. RICHARDSON, AND RODNEY J. WITTLERS

A flume study was conducted to investigate the influence of inflow seepage on localized pier scour through an alluvial channel bed. Eight tests were performed in which seepage inflow ranged from zero to three times the liquefaction velocity of the bed material. Channel Froude numbers ranged from approximately 0.40 to 0.80. The results indicated that for channel Froude numbers less than 0.70 and seepage velocity less than critical, the scour hole degraded by 20 percent. For channel Froude numbers less than 0.70 and seepage velocity greater than critical, the scour hole aggraded while the scour hole width increased as much as 2.25 times wider than scour hole widths observed for the no-inflow conditions. When the channel Froude number exceeded 0.70, scour hole depths were similar to the no-inflow conditions while the bed elevations adjacent to the scour hole significantly degraded.

Localized scour at bridge piers, abutments, and channel banks results in millions of dollars in damage to river-crossing structures. In general, scour is the erosive action of flowing water in streams and rivers that excavates and transports material from channel beds and banks (*10*). Localized erosion often causes a change in the channel bed elevation and/or lateral channel migration into the banks at or near the crossing structure. Improper accounting of many of the site specific parameters affecting local scour may result in a catastrophic failure of the structure.

Several types of local scour can be identified at most river crossings, including constriction scour, abutment scour, aggradation, and degradation. Numerous parameters exist at each river crossing that affects site stability. These parameters may include soil characteristics, hydrologic and hydraulic characteristics, seepage/groundwater conditions, and methods of construction.

A flume study was conducted that measured local scour resulting from flow in a straight alluvial channel around a single circular pier with and without inflow seepage. The objective was to investigate the influence of inflow seepage on localized pier scour and areas adjacent to the pier. Inflow seepage conditions exist when the water table elevation is high enough to contribute flow into the stream through the channel bed and/or banks. It was not the purpose of the study to generate another pier scour prediction equation, but rather to indicate how inflow seepage from the channel bed may affect pier scour prediction. The results are presented in this paper.

BACKGROUND

The attempts to predict the extent of pier scour and enhance bridge design procedures have been studied since the 1940s. One of the most comprehensive literature reviews was conducted by Jones (*10*) in which he cited 12 bridge pier scour prediction equations. Jones categorized the pier scour efforts as (a) pier scour formulas based on foreign research to include Ahmad (*1*), Bruesers (*2*), Chitale (*3*), and Inglis (*8*); (b) pier scour formulas patterned after University of Iowa research to include Laursen (*6–8*) and Jain (*9*); and (c) pier scour formulas patterned after Colorado State University Research to include Shen (*10*) and Richardson, et al. (*11*). All the equations presented were to predict the maximum depth of scour in the area adjacent to the pier. The primary independent variables cited included approach flow depth, projected pier width, approach velocity and Froude number.

Raudkivi performed a comprehensive analysis of flow around a circular pier, concentrating on flow patterns, velocity distributions, variation of scour depths around the pier, scour as a function of sediment gradation, and scour as a function of sediment size (*12*). He concluded that the pier width, type and gradation of sediment, flow depth, sediment size-pier width ratio, and pier alignment control the depth and pattern of scour.

The study of how inflow seepage affects an alluvial channel system has not yielded results as numerically sound as scour prediction. In 1966, Simons and Richardson stated that seepage force could change the bed form and, therefore, the resistance to flow (*13, 14*). However, this was not experimentally or analytically documented in their study. In a qualitative sense, Simons and Richardson concluded that seepage of water into the bed (outflow seepage) would tend to increase the effective weight of the bed particles and, therefore, increase the stability of the bed. Conversely for a gaining stream (groundwater flow into the channel or inflow seepage), the effective weight of the bed particles decreases and thereby decreases the bed stability. The inflow seepage could result in an increase in the sediment transport and change in the predicted bed form. This conclusion was cited in publications by Simons and Richardson (*13*) and Simons and Senturk (*14*).

Martin addressed the influence of inflow and outflow seepage on incipient motion of uniform bed materials (*15, 16*). Martin concluded that inflow seepage does not aid incipient motion of the sediment particles.

Harrison tested the effects of groundwater seepage (inflow, outflow, and zero seepage) forces on sediment transport for both lower and upper regime flows (*17, 18*). Harrison's study indicated that the upward (inflow) seepage had a limited effect on the stream sediment transport rate, even when the bed was quick. He concluded that the decrease in effective grain density brought about by inflow seepage might be offset by a decrease in surface drag on the individual grains and an increase in form drag. Harrison also noted that when bed forms were present the angle of repose of the downstream face of the bed forms increased by 10° for outflow seepage and decreased by 9° for inflow seepage.

Department of Civil Engineering, Colorado State University, Ft. Collins, Colorado 80523.

Harrison (*18*) and Martin (*15*) did not observe a significant increase in sediment transport or scour when inflow seepage occurred. Harrison did note that the bed form could be altered by inflow seepage. However, Harrison did not show that inflow seepage could change the bed form (i.e., from ripples to dunes, dunes to plane, etc.) which was hypothesized by Simons and Richardson (*13*).

The interaction between the channel flow and seepage flow interface and the subsequent response were studied by Watters and Rao (*19*). In their investigation, geometrically packed spheres were analyzed for lift and drag forces under inflow and outflow seepage conditions. Quantitatively, Watters and Rao concluded that inflow seepage tended to reduce the drag on bed particles whether they were on top of or in the soil matrix. The lift on bed particles under inflow seepage increased for particles in the soil matrix, but the lift on particles resting on the bed was reduced.

Watters and Rao concluded that

1. Inflow seepage increased the sublayer thickness.
2. The hydraulic roughness and consequently the drag on the plane bed decreased.
3. Inflow seepage increased the lift on particles within the bed and decreased lift for particles resting on the bed.
4. Turbulent fluctuations were more intense with inflow seepage than for outflow seepage or no seepage.
5. Inflow seepage increased the momentum transfer between fluid particles.

Nezu (*20*) performed a rigorous mathematical analysis quantifying the existence of a matched or exaggerated boundary layer along the bed. Nezu's analysis incorporated turbulence, induced stresses, velocity profiles, and backwater effects on flow over a permeable bed with seepage.

Nezu showed that seepage flow near the porous surface becomes turbulent as a result of the pressure fluctuations of the main flow. When this occurs, the seepage flow cannot remain laminar, and Darcy's law for flow in a permeable medium cannot be applied. This results in an additional shear stress induced in the main flow by the turbulent seepage flow. Nezu identified this additional stress as induced stress.

Richardson et al. conducted a series of tests in which a straight channel with alluvial material was subject to inflow seepage ranging from zero to where the material liquified (*21*). They determined that the bed forms could potentially be altered by inflow seepage. For example, a change from plane bed to ripples to dunes could result from introducing inflow seepage.

Richardson et al. concluded that inflow seepage through a porous bed directly affects many aspects of alluvial channel flow. Inflow seepage influence on the alluvial system is summarized as follows:

1. The interaction between the main and seepage flows causes a boundary layer or wedge to form near the bed. The layer influences the channel hydraulics, bed forms, stream power, and sediment transport in the zone of inflow seepage.
2. The development of the layer or wedge near the bed results in an effective increase in the bed elevation. The water depth decreased by as much as 15 percent for subcritical flow and remained constant for supercritical flow through the inflow seepage zone.
3. The stream power, in the reach where infiltration occurs, increases primarily due to an increase in the water surface slope. The mean velocity was observed to increase as much as 23 percent.
4. Inflow seepage caused significant changes in bed forms and subsequently in the resistance to flow.
5. Fluid shear and fluid particle to particle momentum transfer between the main and seepage flows increase turbulence along the interface.

FACILITIES

The investigation was conducted at the Engineering Research Center at Colorado State University. A 1.5-ft wide (45.7 cm), 2.0-ft (61 cm) deep, and 32-ft (9.8 m) long flume capable of recirculating water and sediment was used for this study. The flume was divided into three reaches. The upstream reach provided a 10-ft (3.0 m) length of channel for the flow, bed forms, surface waves, and sediment transport to stabilize. The upstream reach contained the head box, rock baffle, flow straightener, and wave suppressor. An inflow gallery was located in the mid one-third of the flume. The downstream reach served as an outrun section to minimize the effect of the backwater in the testing zone.

The inflow gallery consisted of perforated pipes installed in the bed of the flume perpendicular to the flow. The length of the inflow gallery was approximately 10 feet (3 m). The perforated pipes, spaced at one foot intervals, were overlain by a one-inch thick layer of one-fourth-inch gravel and a permeable geomembrane to diffuse the seepage flow. A piece of wire mesh was placed on top of the geomembrane and attached the gallery to the flume. Each of the perforated pipes was valved for flow regulation and connected to a common supply conduit.

A single circular pier was used in this study. The pier was 0.104 feet (3.2 cm) in diameter and two feet in length. The pier was placed in the center of the flume 0.75 feet (22.9 cm) from each side wall, and in the center of the inflow gallery, 15 feet (4.6 m) from the flume entrance. The Plexiglas pier extended from the top of the flume, through the flow and bed material, to the top of the wire fabric of the inflow gallery. Channel discharge was measured using a calibrated segmented orifice. Inflow seepage discharge was determined volumetrically. Twelve liters of water were diverted from the inflow discharge supply conduit and the elapsed time recorded. Several measurements of the inflow discharge were made for each test and averaged. The average inflow velocity was determined by dividing the inflow discharge by the area of the inflow gallery.

Water surface slope was measured by the use of three piezometer taps spaced 10 feet (3 m) apart and located on the left wall of the flume. The upstream tap was located in the approach section upstream of the inflow zone. The middle pressure tap was located in the zone of infiltration adjacent to the pier. The third tap was located downstream of the inflow zone.

The mapping of the bed was performed by using a point gauge and a movable carriage on rails mounted on the flume walls. Mapping was performed in cartesian coordinates. Distances in the longitudinal direction are stationed increasing upstream, while the lateral direction represented the distance from the left wall of the flume. The point gauge was capable

TABLE 1 SUMMARY OF DATA

Run	Channel* Discharge Q_c cfs	Mean Channel Velocity V_c fps	Channel Approach Depth d_c ft	Maximum Scour Depth d_{sm} ft	Maximum Scour Width W_{sm} ft	Channel Froude F_c
4-0	1.71	2.02	0.565	0.161	0.53	0.47
1		1.93	0.565	0.183	0.67	0.44
2		1.93	0.608	0.166	1.05	0.44
3		1.93	0.606	0.162	1.17	0.44
5-0	1.50	1.97	0.510	0.200	0.65	0.49
1		1.90	0.502	0.208	0.72	0.46
2		1.90	0.529	0.153	1.11	0.46
3		1.90	0.560	0.105	0.75	0.46
6-0	1.77	2.56	0.461	0.187	0.92	0.66
1		2.33	0.504	0.168	0.91	0.58
2		2.33	0.485	0.159	0.85	0.58
3		2.33	0.531	0.139	1.18	0.58
7-0	1.97	2.45	0.537	0.144	0.98	0.59
1		2.43	0.531	0.162	0.99	0.58
2		2.43	0.538	0.184	0.87	0.58
3		2.43	0.560	0.142	1.06	0.58
8-0	2.10	2.35	0.596	0.178	0.91	0.54
1		2.43	0.605	0.185	0.80	0.57
2		2.43	0.560	0.162	1.03	0.57
3		2.43	0.563	0.137	0.96	0.57
9-0	2.11	2.57	0.550	0.203	0.68	0.61
1		2.21	0.616	0.166	0.79	0.50
2		2.21	0.633	0.166	0.85	0.50
3		2.21	0.671	0.077	0.75	7.50
10-0	1.90	2.36	0.536	0.307	1.00	0.57
1		2.63	0.470	0.142	0.75	0.67
2		2.63	0.489	0.139	0.97	0.67
3		2.63	0.480	0.125	1.06	0.67
11-0	2.11	2.97	0.474	0.138	1.03	0.76
1		3.04	0.463	0.124	0.82	0.79
2		3.04	0.465	0.130	0.86	0.79
3		3.04	0.460	0.125	0.92	0.79

*Water temperature for all tests: 68°F ± 2°F.

of measuring the distance in the vertical direction from a fixed datum to a resolution of 0.001 feet (0.3 mm).

TESTING PROGRAM

A series of eight flume tests were conducted, in which the channel Froude number and the inflow seepage velocity were varied. In each of the eight tests, the channel was subjected to three inflow seepage velocities as well as a no-inflow seepage condition. Table 1 is a tabulation of the channel discharge, average channel velocity, maximum depth of scour, maximum width of scour, and channel Froude number. The run numbers refer to the test and the inflow rate. The inflow rate of zero indicates a no-inflow condition. The inflow rates of 1–3 indicate the range of inflow velocities tested.

The channel discharge varied from 1.504 cubic feet per second (cfs) (0.04 m³/s) to 2.113 cfs (0.06 m³/s). The channel Froude number varied from 0.44 to 0.79. The depth of flow ranged from 0.46 feet (11.3 cm) to 0.67 feet (20.4 cm). The seepage velocities for each test, tabulated in table 2, varied from zero to 2.59×10^{-3} fps (0.08 cm/s). The liquefaction critical seepage velocity for the bed material was 5.4×10^{-4}

TABLE 2 SEEPAGE INFLOW VELOCITIES

Test Number	Inflow Condition 0	1	2	3
4	0	5.00	9.00	11.13
5	0	1.40	10.60	15.73
6	0	2.87	5.40	10.80
7	0	0.60	3.47	9.07
8	0	2.40	4.40	9.33
9	0	3.67	8.13	14.87
10	0	6.33	8.47	15.33
11	0	6.87	15.53	25.87

$v_i * 10^4$ fps

$v_{i_{CR}} = 5.4 \times 10^{-4}$ fps

fps (0.016 cm/s) and shall be referenced as the critical or threshold inflow velocity.

MATERIAL

The alluvial bed material was a silica river sand. A visual accumulation tube analysis (VA) was performed to determine the fall diameter of the material. The VA analysis determined the material to have a fall diameter of 0.27 mm. A sieve analysis indicated that the median grain size of the material was 0.33 mm. The VA and sieve analysis were performed after the material had been washed.

TESTING PROCEDURE

At the beginning of each test run, the channel discharge was established and the flume adjusted to produce a flow depth of approximately 0.5 ft (15.2 cm). The sediment depth was approximately 0.7 ft. The flume was then allowed to run a minimum of 12 hours to stabilize flow conditions relative to discharge and sediment recirculation in the channel. Stability of flow was subjectively judged to have been established when the bed elevation was steady for a period of at least one hour.

Data were collected after flow and sediment stabilization. Sediment transport rates were not measured. These data included the channel discharge, inflow discharge, water surface slope, and the mapping of the bed. After initial data collection, the inflow seepage was either initiated or increased. The channel was allowed to restabilize for a period of two to six hours and data were again collected.

The first data collection was conducted without inflow seepage. Subsequent subtests were conducted with inflow seepage as shown in table 2. The zero inflow test data were used to form a baseline to compare the influence of inflow seepage on scour around the pier. The higher seepage rates were sufficient to cause localized liquefaction of the bed material.

Flow depth was measured during the mapping of the bed. Cross sections were located upstream and downstream of the pier at 0.10-ft (3 cm) intervals. In each cross section, vertical elevations of the bed were measured every 0.2 feet (6.1 cm) or at each break in grade. At each cross section, water level readings were taken along with the measurements of the bed elevation. The difference between these measurements yielded the flow depth at each cross section. The water temperature for all tests was 68° ± 2°.

RESULTS

The initial step in the analysis was to compare the equilibrium scour depths obtained in this study with composite data presented by Jones (*10*). Figure 1 portrays the scour depths versus pier Reynolds number relationship. The scour depths resulting from the eight record tests for the no inflow condition are shown in figure 1. Although the maximum scour depths plot below the prediction relationship, the no-inflow scour depth data fall well within the data scatter of previous studies. Therefore, these test results compare favorably with accepted procedures for estimating pier scour depth.

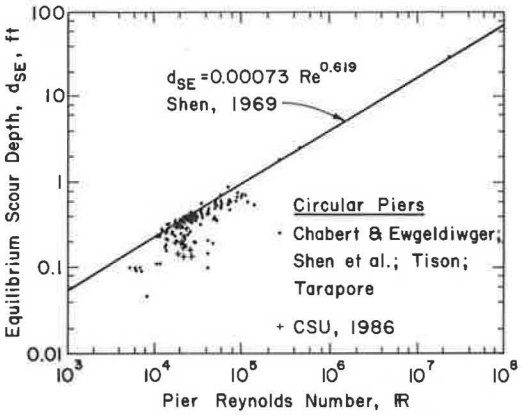

FIGURE 1 Scour depth versus pier Reynolds number (after Shen).

Scour Depth

During each test, the depth of scour was carefully monitored for each no-inflow and inflow seepage condition. The maximum scour depths, d_{sm}, adjacent to the circular pier without seepage inflow are presented in table 1. The maximum scour depths recorded without seepage inflow were compared to the maximum scour depths recorded with varying inflow seepage conditions. A typical longitudinal section relating the maximum scour depths of the no-inflow condition to the maximum inflow seepage condition is presented in figure 2 for test 10. It is observed in figure 2 that the presence of inflow seepage resulted in a decrease in the maximum depth of the scour hole. The decrease in scour hole depth in the presence of inflow seepage was observed for tests where the Froude number ranged from 0.4 to 0.7. In general, as the inflow seepage velocity rate increased, the maximum depth of scour became shallower. The data indicate that when the measured inflow seepage rate, v_i, exceeded the critical inflow seepage, v_{iCR}, rate by a factor of 3, the maximum scour hole depth decreased by 62 percent.

In order to trace the development of the pier scour depth, the ratio of the maximum scour depth with inflow to the

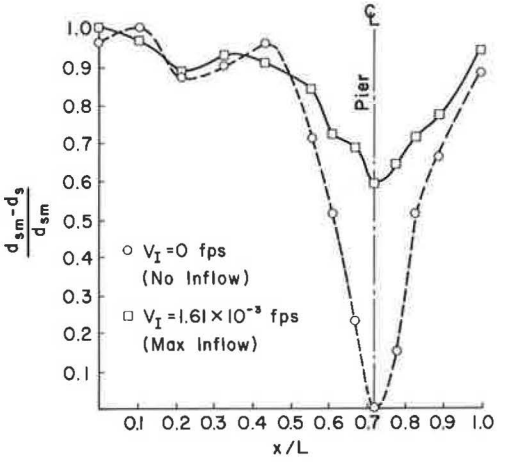

FIGURE 2 Longitudinal section for test run No. 10, L = 2.3 ft.

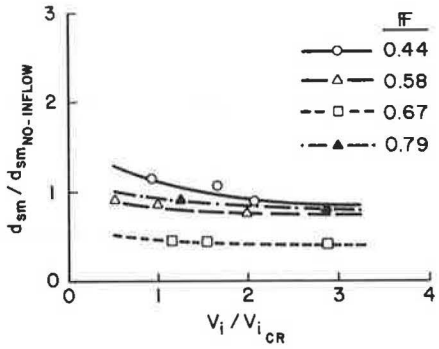

FIGURE 3 Pier scour depth as a function of inflow seepage and channel Froude number.

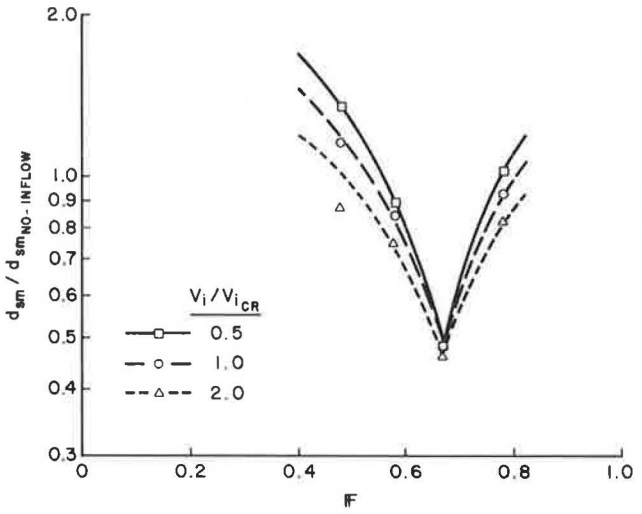

FIGURE 4 Pier scour depth versus channel Froude number.

maximum scour depth without inflow was related to the ratio of the inflow seepage velocity to the critical inflow seepage velocity as presented in figure 3. It is observed that when the Froude number ranges from 0.44 to 0.67, the pier scour depth decreases as the inflow seepage velocity increases. The maximum depth of scour with inflow seepage exceeded the maximum scour depth without inflow seepage by 20 percent when the channel Froude number was less than approximately 0.5 and the inflow seepage velocity was less than liquefaction. However, the trend is reversed when the Froude number exceeded 0.70. The trend reversal becomes evident where the depth of pier scour is related to the channel Froude number, as shown in figure 4. When the channel Froude number approached 0.7, the scour depth ratio converged at approximately 0.48, independent of inflow seepage velocity. The maximum scour depth then increased as the Froude number and the inflow seepage velocity increased. The scour hole depth degraded toward the no-inflow scour depth level.

Scour Width

The width of scour adjacent to the circular pier was measured and documented as shown in table 1 for each test. It is observed that for the tests in which the channel Froude number is less than 0.70, the maximum width of scour, W_{sm}, with inflow seepage exceeds the maximum width of scour without inflow seepage. An example of how inflow seepage affects the maximum width of scour is illustrated in figure 5. Figure 5 shows the bed and scour hole elevations relative to the maximum scour depth without inflow seepage at a cross section immediately downstream of the pier for test 9. Without inflow seepage, the scour hole was localized and well defined. When inflow seepage was introduced, the scour hole filled and the

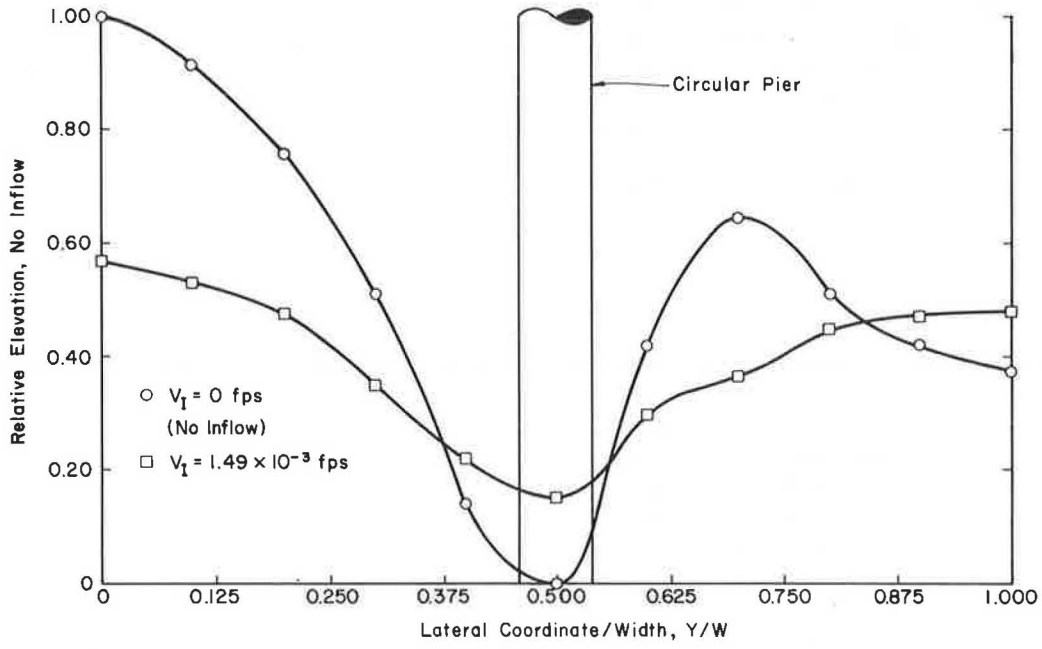

FIGURE 5 Inflow seepage influence on scour width.

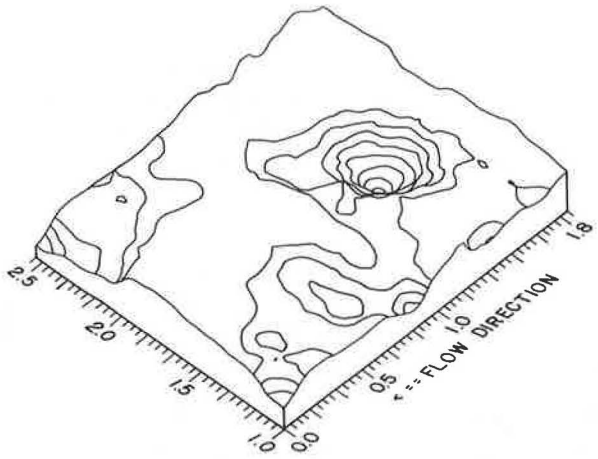

FIGURE 6 Alluvial bed topography for test 5, no inflow.

hole side slopes flattened. As the seepage rate increased, the width of scour increased. The presence of inflow seepage reduced the bed elevation relative to the maximum depth of scour by as much as 50 percent at a lateral distance of 8 pier diameters away from the pier. The flattened bed resembled a general scour condition between piers.

A series of topographic plots were constructed to illustrate the widening of the scour hole as shown in figures 6–9. The alluvial bed topography for test 5 indicates the general scour conditions that resulted from seepage inflow when inflow ranged from zero, Figure 6, to 290 percent of the liquefaction velocity, Figure 9.

In an attempt to correlate the maximum scour hole width, W_{sm}, to the inflow seepage velocity, v_i, and channel Froude numbers, the ratio of the maximum scour width with inflow seepage divided by the maximum scour width without inflow seepage (W_{sm} no-inflow) was related to the ratio of inflow seepage velocity divided by the critical inflow seepage velocity, as presented in figure 10. It is observed that for channel Froude numbers less than or equal to 0.50, inflow seepage increases scour hole widths by as much as 2.25 times the no inflow seepage condition. However, as the inflow velocity increases and the channel Froude number increases, the scour hole width decreases, as shown in figure 11.

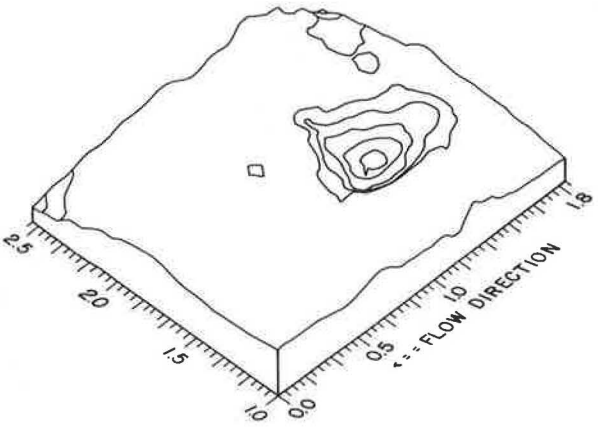

FIGURE 7 Alluvial bed topography for test 5, inflow at 25 percent of liquefaction velocity.

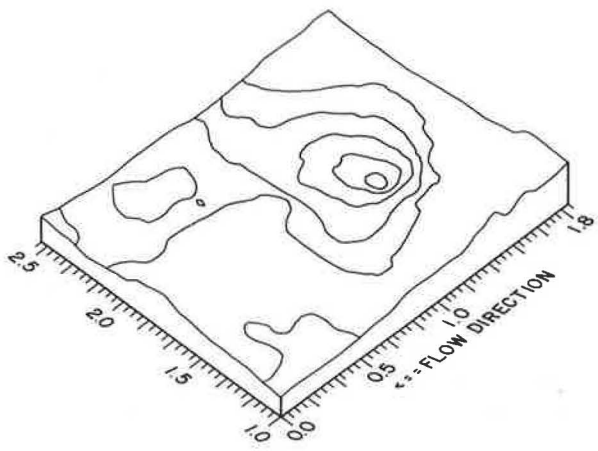

FIGURE 8 Alluvial bed topography for test 5, inflow 200 percent of liquefaction velocity.

GUIDELINES

Based on the test results and analysis, it appears that the presence of inflow seepage alters the extent of localized pier scour in an alluvial channel. The following guidelines are presented in accordance with these findings:

Seepage Influence on Scour Depth

F < 0.70 scour hole may aggregate up to 60 percent of the no-inflow condition if $V_i < V_{CR}$

F < 0.70 scour hole may degrade 20 percent if $V_i < V_{CR}$

F ≥ 0.70 scour hole degradates toward no-inflow level

Seepage Influence on Scour Width

F < 0.5 scour width may increase by 2.25 times over the no seepage condition

F < 0.7 adjacent bed elevations may degradate to 50 percent of the difference between the maximum scour depth and bed elevation for the non-inflow condition

F < 0.7 little difference between the inflow and the no-inflow conditions.

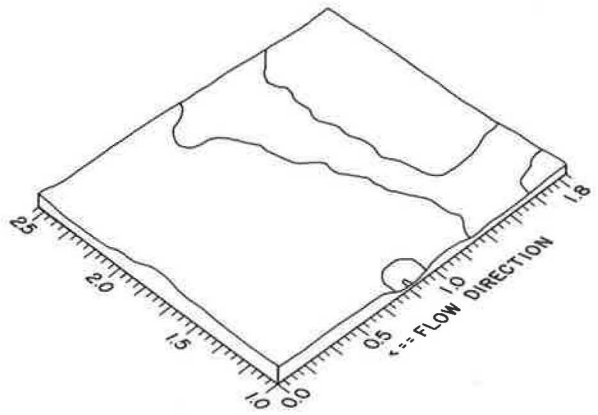

FIGURE 9 Alluvial bed topography for test 5, inflow at 290 percent of liquefaction velocity.

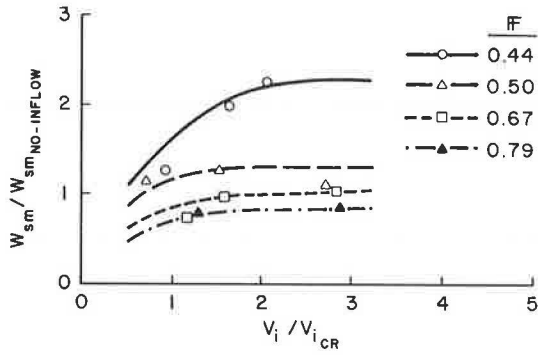

FIGURE 10 Relative scour width as a function of inflow seepage and channel Froude number.

These guidelines are based on tests in which channel Froude numbers range from 0.4 to 0.8 and inflow seepage velocities range from 0.5 to 3.0 times the critical inflow seepage velocity. Further, only a single circular pier was tested.

APPLICATIONS

It is recommended that all bridge sites be evaluated for the presence of inflow seepage. If inflow seepage is found or suspected, it would be prudent to increase the predicted pier scour hole depth independent of scour estimation procedure by approximately 20 percent. The presence of inflow seepage escalates the risk of increased scour around the pier. Also, the presence of inflow seepage can potentially increase the width of pier scour by 225 percent over no-inflow conditions. Although these guidelines reflect worst-case scenarios, they represent a real risk to existing and planned structures.

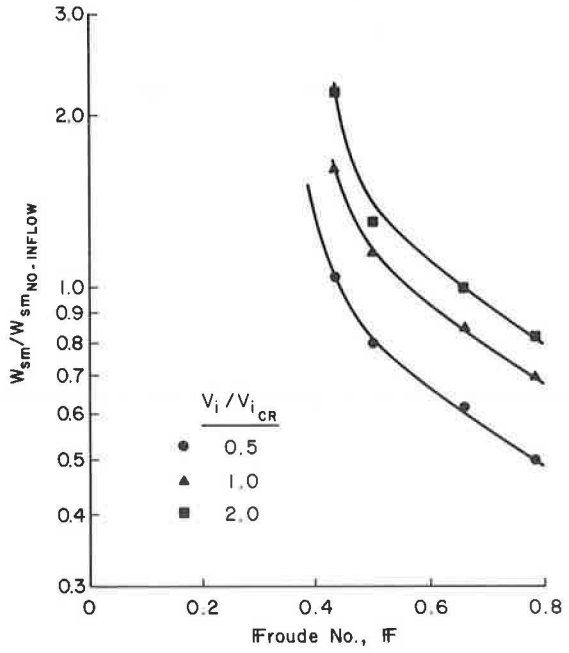

FIGURE 11 Scour width versus channel Froude number with varying inflow seepage conditions.

CONCLUSIONS

Inflow seepage significantly affects scour hole depth at piers. When the channel Froude number is less than 0.7 and the inflow seepage velocity is less than critical, the scour hole depth may increase by 20 percent over the no-inflow seepage scour depth. When the Froude number is less than 0.7 and the seepage velocity is greater than the critical seepage velocity, the scour hole depth decreases by 60 percent over the no-inflow seepage scour depth. When channel Froude numbers exceed 0.7 and inflow seepage is present, the scour depth decreases by 40 to 60 percent of the no-inflow maximum scour depth. General bad degradation occurs as seepage velocity increases.

The scour hole width may increase by 225 percent over the no-inflow seepage condition for Froude numbers of less than or equal to 0.5. The increase in scour hole width is attributed to the general bed degradation as the bed washes out.

REFERENCES

1. J. Jones. Comparison of Prediction Equations for Bridge Pier and Abutment Scour. *Transportation Research Record 950*, Vol. 2, 1984, pp. 202–208.
2. M. Ahmad. Discussion of "Scour at Bridge Crossings," by E. M. Laursen, *Transactions of the ASCE*, Vol. 127, 1962, pp. 198–206.
3. H. N. C. Bruesers. Scour Around Drilling Platforms. *Bulletin Hydraulic Research 1964 and 1965*. International Association for Hydraulic Research, Delft, Netherlands, Vol. 19, p. 276, 1965.
4. S. V. Chitale. Discussion of "Scour at Bridge Crossings," by E. M. Laursen, *Transactions of the ASCE*, Vol. 127, pp. 191–196, 1962.
5. C. C. Inglis. *The Behavior and Control of Rivers and Canals*. Research Publication 13, Central Power, Irrigation and Navigation Report, Poona Research Station, India, 1949.
6. E. M. Laursen. Scour at Bridge Crossings. Bulletin 8, Iowa Highway Research Board, *Transactions of the ASCE*, Vol. 127, 1962.
7. E. M. Laursen. An Analysis of Relief Bridge Scour. *Journal of the Hydraulic Division of the ASCE*, Vol. 89, No. HY3, May 1969.
8. E. M. Laursen. *Scour Around Bridge Piers and Abutments*. Bulletin 4, Iowa Highway Research Board, Iowa City, May 1956.
9. S. C. Jain and E. E. Fisher. *Scour Around Circular Bridge Piers at High Froude Numbers*. Report FHWA-RD-79-104, FHWA, U.S. Department of Transportation, April 1979.
10. H. W. Shen, V. R. Schneider, and S. S. Karaki. Local Scour Around Bridge Piers. *Journal of the Hydraulic Division of the ASCE*, Vol. 89, November 1969.
11. *Highways in the River Environment: Hydraulic and Environmental Design Considerations*. FHWA Training and Design Manual, Civil Engineering Department, Colorado State University, U.S. Department of Transportation, May 1975.
12. A. J. Raudkivi. Functional Trends of Scour at Bridge Piers. *ASCE Journal of Hydraulic Engineering*, Vol. 112, No. 1, January 1986, pp. 1–13.
13. D. B. Simons and E. V. Richardson. *Resistance to Flow in Alluvial Channels*. U.S. Geological Survey Professional Paper 422-J, 1966.
14. D. B. Simons and F. Senturk. *Sediment Transport Technology*, Water Resources Publications, Fort Collins, Colorado, 1977.
15. C. S. Martin. Effects of a Porous Sand Bed on Incipient Sediment Motion. *Water Resource Research*, Vol. 6, No. 4, 1970, pp. 1162–1174.
16. C. S. Martin. *The Effect of a Permeable Bed on Sediment Motion, Phase I: Seepage Force on Bed Particles*. Final Report, OQRT Project No. B-004-GA, 1966.
17. S. S. Harrison. The Effects of Groundwater Seepage on Stream Regime—A Lab Study. M.S. thesis. University of North Dakota, 1968.

18. S. S. Harrison and L. Clayton. Effects of Groundwater Seepage on Fluvial Processing. *Bulletin of the Geological Society of America*, No. 811, 1970, pp. 1217–1225.
19. G. Z. Watters and M. V. P. Rao. Hydrodynamic Effects of Seepage on Bed Particles. *Journal of the Hydraulic Division*, ASCE, Vol. 97, No. HY3, Proc. Paper 7873, 1971, pp. 421–439.
20. I. Nezu. Turbulent Structure in Open Channel Flows. Thesis. Kyoto University, Japan, 1977.
21. J. R. Richardson, S. R. Abt, and E. V. Richardson. Inflow Seepage Influence on Straight Alluvial Channels. *Journal of Hydraulic Engineering*, Vol. 111, No. 8, August 1985, pp. 1133–1147.